Journal of Holography Applications in Physics
Volume 6, Issue 2, Spring 2026, 104–118
©Available online at http://jhap.du.ac.ir
DOI: 10.22128/jhap.2025.3147.1161
Online ISSN: 2783–3518

Regular article

Gravitational Lensing by Kalb-Ramond Black Holes Coupled by Nonlinear Electrodynamics

Aadya Sharma · Bablu · Dharm Veer Singh

[1] Department of Physics, Institute of Applied Science and Humanities, GLA University, Mathura 281406, India;
Corresponding Author E-mail: aadyasharma012@gmail.com

[2] Department of Physics, Institute of Applied Science and Humanities, GLA University, Mathura 281406, India;
E-mail: babluchaudhary0003@gmail.com

[3] Department of Physics, Institute of Applied Science and Humanities, GLA University, Mathura 281406, India;
E-mail: veerdsingh@gmail.com

Received: November 16, 2025; **Revised:** December 15, 2025; **Accepted:** December 22, 2025

Abstract. In this paper, we study the black hole solution coupled with the Kalb–Ramond (KR) field and nonlinear electrodynamics (NLED). The obtained black hole solutions interpolate between a Kalb-Ramond black hole in the absence of NLED and the Schwarzschild black hole in the limit of vanishing KR and NLED field. We study gravitational lensing by a black hole solution. In addition, we estimate the mass parameter and constrain it using observational data.

Keywords: Black Holes; Kalb Ramond Gravity; Gravitational Lensing.

Contents

1 Introduction

General Relativity is a theory of gravity given by Albert Einstein in 1915, which is now used as a standard depiction of modern physics [1]. Previously gravity was understood as a force but general relativity redefined our understanding of gravity as the curvature of space and time due to mass and energy. In 1919 Eddington validated it by observing the total solar eclipse [2] and Event Horizon Telescope (EHT) Collaboration give the first-ever image of the M87 galaxy [3–11]. The bending of light rays due to the presence of matter (massive objects) manifests as gravitational lensing. Virbhadra and Ellis elucidated the gravitational lensing produced by a Schwarzschild black hole [12,13]. The Gravitational lensing can occur in three ways: strong, weak and micro lensing. The Strong lensing occurs due to massive bodies and the images formed can be resolved and there must be close alignment between lens and the source. Weak lensing occurs when the lens is not so powerful and the images formed are distorted but magnified and the Micro lensing occurs due to small lenses like stars and exoplanets. There are many studies of gravitational lensing for the solution presented in refs [14–19].

On the theoretical side, the study of Lorentz symmetry breaking (LSB) is important for understanding quantum gravity processes in fundamental physics [20–24]. An example of a LSB is the Bumblebee gravity theory [25] and another example is the Kalb Ramond (KR) gravity theory, which incorporates a nonminimally coupled tensor field $B_{\mu\nu}$, known as the KR field [26]. The string theory suggests that this symmetry might break at very high energies. In string theory, the particles are replaced with tiny vibrating strings. The KR field couples naturally to these strings similarly as electromagnetic vector potential couples to point particles.

In this paper, we generalize regular black hole in KR gravity. The Bardeen black hole is regular black hole (center singularity is absent) is proposed by Bardeen based on the Sakharov [27] and Gliner proposal [28] and 30 year later an exact solution of Bardeen black hole [29] was obtained when gravity is coupled with nonlinear electrodynamics (NLED) [30–33]. There are many black hole solution based on Bardeen [34–48]. In this work we focus on strong field limit of Bardeen black hole in KR field and analyze it's lensing observables.

The paper is organized as follows, we obtain an exact black hole solution in the presence of KR gravity coupled with NLED in Sec. 2, and study the location of the horizon structure. The study of the unstable circular orbit of obtained black hole solutions in the Sec. 3. The Sec. 4 is devoted to study the observable of the Bardeen KR black hole in the strong field limit including Einstein ring and magnification. Finally, the concluding remarks and results are presented in Sec. 5.

2 Kalb-Ramond field for regular black holes

In this section, we discuss a regular black hole solution in the field limit of KR. The KR gives a breaking of Lorentz symmetry. We are considering a spherically symmetric and static black hole solution in this field limit.

$$ds^2 = -A(r)dt^2 + \frac{dr^2}{A(r)} + C(r)d\Omega^2, \tag{2.1}$$

with

$$A(r) = \frac{1}{1-l} - \frac{2Mr^2}{(r^2+g^2)^{3/2}}, \tag{2.2}$$

where, $d\Omega^2 = d\theta^2 + \sin^2\theta d\phi^2$ where l denotes Lorentz symmetry violation effect by KR field's non - zero vacuum expectation value and it is a dimensionless quantity. To find the horizons of this black hole solution, we find roots by $A(r) = 0$. The roots or zeroes means the curve cuts the r axis and the number of crossing shows the number of roots. Here, we get two real roots from $A(r) = 0$ which corresponds to Cauchy and Event Horizon.

As we can observe, the metric (2.1) has a coordinate singularity at $A(r) = 0$, which results in two real roots as follows:

$$r = \pm\frac{1}{\sqrt{6}}\sqrt{\frac{\sqrt[3]{2}\left(2A^4 - 12A^2g^2 + \sqrt[3]{2}B^{2/3}\right)}{\sqrt[3]{B}} - 6g^2 + 2(A)^2}, \tag{2.3}$$

where $B = 2A^6 - 18A^4g^2 + 27A^2g^4 + 3\sqrt{81A^4g^8 - 12A^6g^6}$, and $A = l - 1$.

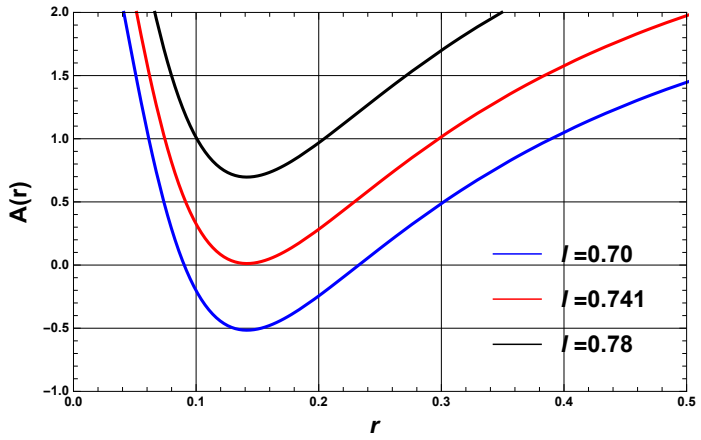

Figure 1: Plots of $f(r)$ vs r for different values of l with fixed values of magnetic charge (g).

Fig. 1 has horizon plots in which we use variation of l with fixed parameters magnetic charge $g = 0.1$. We can observe from Fig. 1, that the size of the black hole decreases with an increase in l. We calculate equation of motion and effective potential for this black hole solution. We consider a spacetime which is spherically symmetric. Time-like killing vector $(\partial/\partial t)^\mu$ corresponding to time translation and space-like killing vector $(\partial/\partial\phi)^\mu$ corresponding to spatial rotations and $(\theta = \pi/2)$ is considered an equatorial approximation.

3 Unstable Circular Orbit

The motion should satisfy the constraint $g_{\mu\nu}\dot{x}^\mu\dot{x}^\nu = -k$, where value of k can be 1 or 0 for massive and massless particles respectively. As we consider spacetime to be spherically symmetric, it can be assumed that at equatorial surface $\theta = \frac{\pi}{2}$ the movement takes place. As the metric does not depend on either t or ϕ, the conjugates of t and ϕ give two constants of motion. The energy and angular momentum of the particle can be calculated as follows

$$E = A(r)\dot{t}, \tag{3.1}$$

$$L = r^2\dot{\phi}. \tag{3.2}$$

For the null geodesic equation i.e., $ds^2 = 0$ and using Eqs.(3.1) and (3.2), we get the relation of the effective potential with the radial motion of the photons or particle moving around

the black hole as follows,

$$\dot{r}^2 = E^2 - L^2 \frac{A(r)}{C(r)}. \tag{3.3}$$

The radial effective potential $V_{eff} = L^2 \frac{A(r)}{C(r)}$, given as

$$\frac{L^2}{r^2}\left(\frac{1}{1-l} - \frac{2Mr^2}{(r^2+g^2)^{3/2}}\right). \tag{3.4}$$

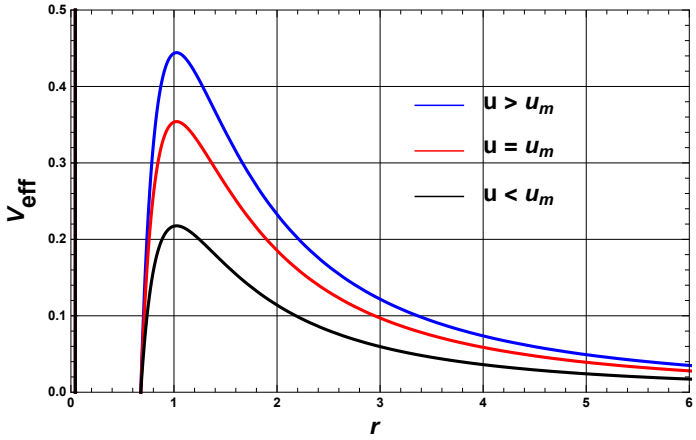

Figure 2: Plots of V_{eff} vs r for varying impact parameter,u with constant values of magnetic charge g. and l

In gravitational lensing, a particle will reach a distance i.e. distance of minimum approach (r_0) from gravitational lens before being deflected by gravitational pull of the lens. For such distance, we relate this with impact parameter, which is denoted by u with closest distance as shown below

$$u = \sqrt{\frac{C(r_0)}{A(r_0)}}. \tag{3.5}$$

For photons oscillating close to the black hole, the turning point of the particle i.e., $\dot{r} = 0$, and the photon sphere radius r_m can be calculated from

$$\frac{A'(r)}{A(r)} = \frac{C'(r)}{C(r)}. \tag{3.6}$$

The above equation Eq. (3.6) have at least one real solution and then the largest real value defines the radius of the unstable circular photon orbits. The value of the impact parameter $u = u_m$ for radius r_m defines the value of critical impact parameter. For calculating the value of deflection angle in strong field limit, a method is developed by Bozza [49]. According to it, the total deflection angle by the light from source to observer is given as

$$\alpha(r_0) = I(r_0) - \pi, \tag{3.7}$$

where $I(r_0)$ is

$$I(r_0) = 2\int_{r_0}^{\infty} \frac{d\phi}{dr}\, dr = \int_{r_0}^{\infty} \frac{2dr}{\sqrt{A(r)C(r)}\sqrt{\frac{C(r)A(r_0)}{C(r_0)A(r)} - 1}}. \tag{3.8}$$

According to Bozza [49] we expand the deflection angle near the photon sphere, for this we define a new variable z as

$$z = \frac{A(r) - A(r_0)}{1 - A(r_0)}, \tag{3.9}$$

the integral (3.7) can be rewritten as

$$I(r_0) = \int_0^1 R(z, r_0) f(z, r_0) dz, \tag{3.10}$$

in which the function $R(z, r_0)$ is

$$R(z, r_0) = \frac{2\sqrt{C(r_0)}(1 - A(r_0))}{C(r)A'(r)}, \tag{3.11}$$

and it remains as regular for every value of z and r_0. The function $f(z, r_0)$ is

$$f(z, r_0) = \frac{1}{\sqrt{A(r_0) - \frac{A(r)}{C(r)}C(r_0)}}, \tag{3.12}$$

where $r = A^{-1}[(1 - A(r_0))z + A(r_0)]$. By Taylor series expansion for function from Eq. (3.12), we get

$$f_0(z, r_0) = \frac{1}{\sqrt{\lambda 1(R_0)z + \lambda 2(r_0)z^2}}, \tag{3.13}$$

where

$$\lambda 1(r_0) = \frac{1 - A(r_0)}{A'(r_0)C(r_0)}[C'(r_0)A(r_0) - A'(r_0)C(r_0)], \tag{3.14}$$

$$\lambda 2(r_0) = \frac{(1 - A(r_0))^2}{2A'(r_0)^3 C(r_0)^2}\left[2C(r_0)C'(r_0)A'(r_0)^2 + A(r-0)A'(r_0)C(r_0)C"(r_0) - C(r_0)C'(r_0)\right]. \tag{3.15}$$

The integrand term $f(z, r_0)$ diverges for $r_0 \to r_m$ leading to diverging deflection angle in Eq. (3.10). To remove this divergence, we used Taylor series expansion and subtracted this divergence term from $I(r_0)$ to get the regular term $I_R(r_0)$. $R(z, r_0)$ is regular for all values of z. Following the above definitions, the diverging part in the integral Eq. (3.10)can be expressed as

$$I_D(r_0) = \int_0^1 R(0, r_m) f(z, r_0) dz, \tag{3.16}$$

and the regular part $I_R(r_0)$ is defined as

$$I_R(r_0) = I(r_0) - I_D(r_0) = \int_0^1 \left(R(z, r_0)f(z, r_0) - R(0, r_m)f(z, r_0)\right) dz, \tag{3.17}$$

where $I_D(r_0)$ shows logarithmic divergence and $I_R(r_0)$ is regular with divergence subtracted from the complete integral (3.10). We calculate the value of deflection according to [49]

$$\alpha_D(r_0) = \bar{a}\log(\frac{r_0}{r_m} - 1) + \bar{b} + O(r_0 - r_m), \tag{3.18}$$

where

$$\bar{a} = \frac{R(0, r_m)}{2\sqrt{\lambda 2(r_m)}}, \tag{3.19}$$

$$\bar{b} = -\pi + I_R(x_m) + \bar{a}\log\left(\frac{2\lambda 2(r_m)}{Ar_m)}\right), \tag{3.20}$$

The Eq. (3.18) can be expressed by using a coordinate independent variable, impact parameter u, as follows

$$\alpha(u) = -\bar{a}\log\left(\frac{u}{u_m} - 1\right) + \bar{b} = O(u - u_m), \tag{3.21}$$

where $\bar{a}$ and $\bar{b}$ defines the strong deflection limit coefficients.

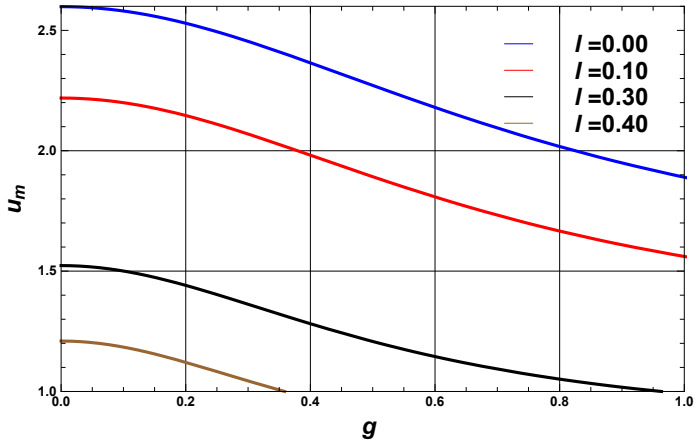

Figure 3: Plot for photon circular orbit, impact parameter u_m vs g with different values of l.

In Fig. 3, we plot the impact parameter u_m for the photons moving on the unstable circular orbits around the black hole. In Fig. 3, we observe u_m decreases with l. In Fig. 4 the deflection angle $\alpha_D(u)$ is plotted with various values of l and the deflection angle as a function of the impact parameter u. In Fig. 4 deflection angle decreases with increasing l.

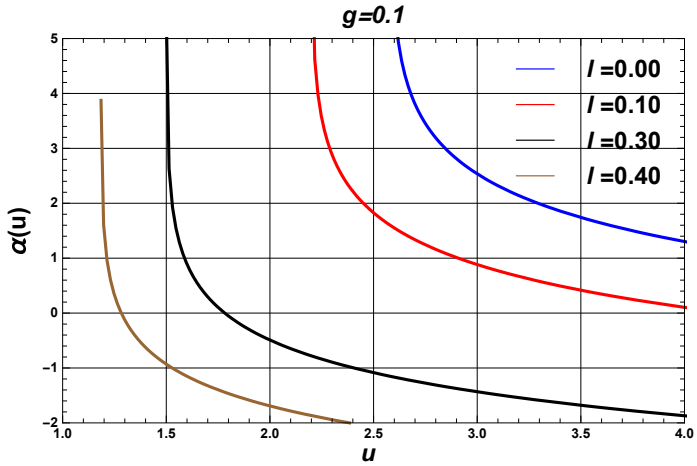

Figure 4: The plot of deflection angle for magnetic charge, $g = 0.1$. as a function of impact parameter, u

4 Observables

We have calculated the deflection angle using Eq. (3.21), we can find the image positions using Virbhadra-Ellis lens equation [12]. The lens equation has an observational setup of gravitational lensing, the position of observer O, black hole L, the source S and the position of image due to lensing in a given coordinate system can be calculated as [12]

$$D_{OS}\tan\beta = \frac{D_{OL}\sin\theta - D_{LS}\sin(\alpha-\theta)}{\cos(\alpha-\theta)}, \tag{4.1}$$

where β and θ denotes the angular separation among image and source of black hole. The distance between black hole and source, observer and source, observer and black hole are D_{LS}, D_{OS} and D_{OL} respectively. Considering small values of Θ and β for perfect alignment of source, black hole and observer, then Eq. (4.1 can be simplified to,

$$\beta = \theta - \frac{D_{LS}}{D_{OS}}\Delta\alpha_n. \tag{4.2}$$

In above equation $\Delta\alpha_n$ defines deflection angle for the nth image

$$\theta_n = \theta_n^0 + \frac{(D_{OL}+D_{LS})}{D_{LS}}.\frac{u_m e_m}{D_{OL}\bar{a}}(\beta-\theta_n^0). \tag{4.3}$$

4.1 Einstein Ring

It has been observed that when a source is placed in front of the lens, it could produce relativistic images and form Einstein Rings.[12] When the lens, source and observer are perfectly aligned in presence of strong gravitational lensing, conditions are met and Einstein rings are formed. We can calculate the Einstein rings position using $\beta = 0$ and $D_{OS} = 2D_{OL}$, θ_n^0 as some reference initial position for image from either side of the lens as follows

$$\theta_n^E = \frac{u_m}{D_{OL}}(1+e_n), \tag{4.4}$$

where e_n as

$$e_n = e^{\frac{\bar{b}}{\bar{a}} - \frac{2n\pi}{\bar{a}}}. \tag{4.5}$$

Eq. (4.4) gives radii of rings of the nth relativistic Einstein ring. Here $n = 1$ gives the outermost ring. The Einstein ring size decreases for the higher order of n, where n is an integer except 0. As the distance between observer and lens increases, the Einstein ring size decreases. In the case of massive black holes, the Einstein ring size becomes large. Due to strong lensing, there are infinitely many apparent images formed for the actual source and because of their large number, these images appear in form of rings.

In Fig. 5 we have plotted the Einstein rings of two astrophysical black holes, SgrA*, and M87*, respectively. It is observed that angular radius for both black hole decreases due to parameter l and the radius of the Einstein ring increases as mass of the object increases and is hence directly proportional. In Fig. 5 it clear that angular radius for SgrA* is grater than M87*.

4.2 Magnification

Magnification is another source of information in strong field limit observable. It is defined as the ratio between the solid angles subtended by the image to the solid angles subtended

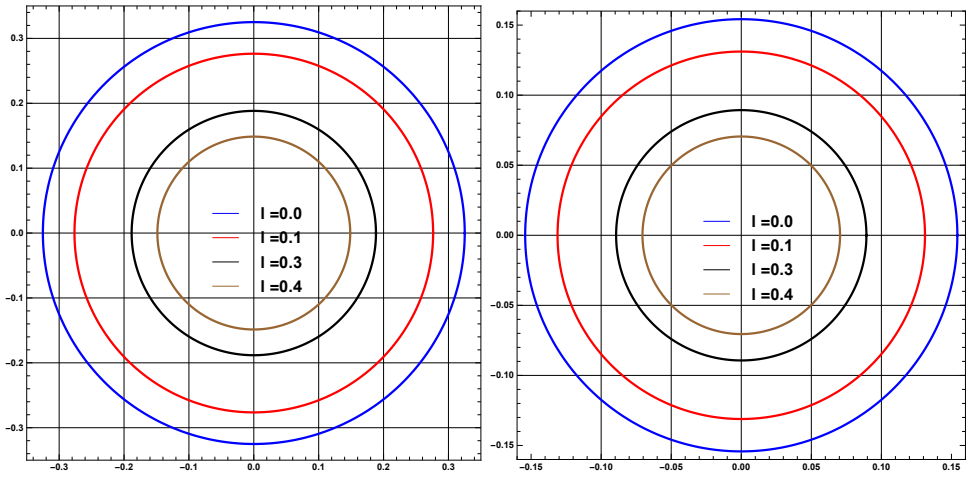

Figure 5: The plots of Einstein rings for astrophysical black hole SgrA*(left) and M87*(right) with fixed value of magnetic charge (g).

by the source, and is determined by the following relation,

$$\mu = \left(\frac{\sin\beta\partial\beta}{\sin\theta\partial\theta}\right)^{-1}. \tag{4.6}$$

Using Eqs. (4.2) and (4.5), the magnification is expressed in the context of strong deflection limit coefficients is given by

$$\mu_n = \frac{1}{\beta}\left[\frac{u_m}{D_{OL}}(1+e_n)\left(\frac{D_{OS}u_m e_n}{D_{LS}D_{OL}\bar{a}}\right)\right]. \tag{4.7}$$

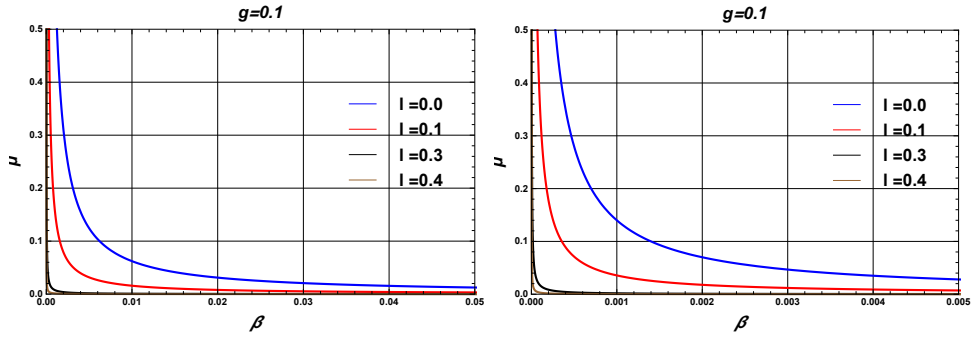

Figure 6: Magnification for fixed value of magnetic charge, g for astrophysical black hole M87*(right) and SgrA*(left) with position of source β.

In Fig. 6 it is observed that the magnification is inversely proportional to the position of the source and magnification diverges when the position of the source approaches zero. From Fig. 6 we can verify that magnification of M87* is small as compared to the magnification of SgrA*. For relating analytical results with observations, we use the observables defined by Bozza [49] as follows,

$$\theta_\infty = \frac{u_m}{D_{OL}}, \tag{4.8}$$

$$s = \theta_\infty(e^{\frac{\bar{b}-2\pi}{\bar{a}}}), \tag{4.9}$$

$$r_{mag} = e^{\frac{2\pi}{\bar{a}}}, \tag{4.10}$$

here s defines the angular separation among the outermost image formed from the rest of the images, r_{mag} defines the ratio of received flux of first image to the received flux of rest of the images clustered at θ_∞. Here, θ_∞ is known as the position of the innermost packed image and is defined as the angular radius of the photon sphere.

In comparison to Schwarzschild black hole, the angular separation observed between images are relatively higher and the magnification is relatively lower. Whereas when fixed value parameters are considered, Sgr A* black hole shows relatively higher angular separation as compared to M87* black hole. In Figs. 7 and 8 we plotted lensing observables θ_∞ and s versus magnetic charge g for both astrophysical black hole SgrA* and M87*. The limiting value for angular position θ_∞ decreases with l and is lower than that of a Schwarzschild black hole. In case of of separation between the image, s, for Kd is larger than the Schwarzschild black hole and it further increases with l.

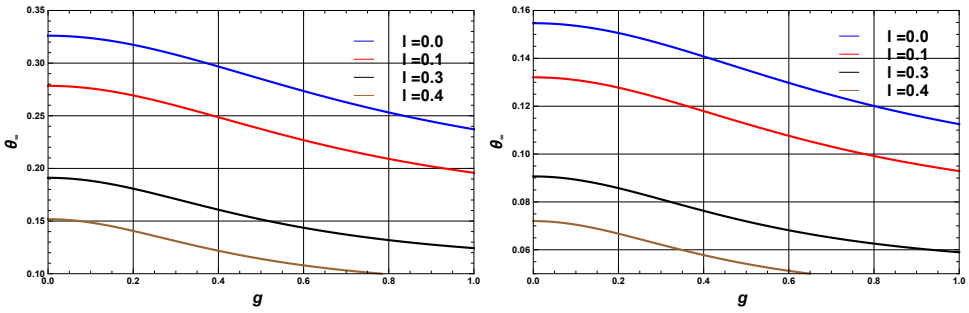

Figure 7: Plots showing the behavior of observables for strong lensing, θ_∞ of astrophysical black hole M87*(right) and SgrA*(left) versus magnetic charge g with variation of l.

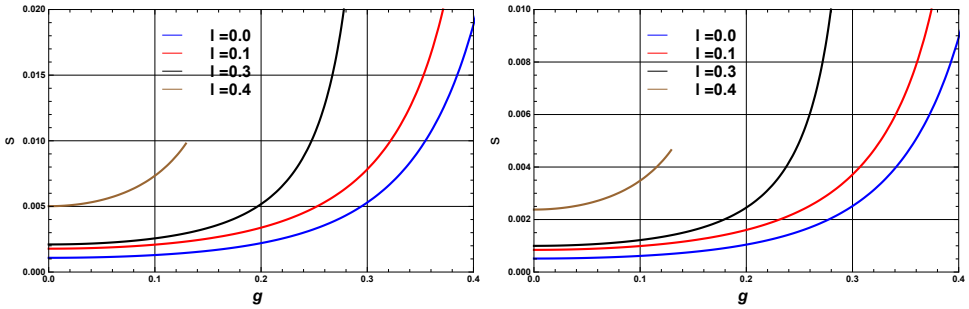

Figure 8: Plots showing the behavior of observables for strong lensing , s of astrophysical black hole M87*(right) and SgrA*(left) vs magnetic charge (g) with variation of l.

5 Conclusions

The gravitational lenses generated by black hole described by KR with Bardeen modification in KR field limit in which LSB implemented with parameter l are studied. We first

demonstrated the solution and plotted a horizon plots for KR modified field limit. Further we proceed to the equations of motion and effective potential V_{eff} in Fig. 2 is a radial effective plot. We calculated the deflection angle α_D and strong lensing coefficients $\bar{a}$ and $\bar{b}$. Furthermore, we have applied the results to lensing observables and plotted these plots in Fig. 6, 7 and 8 for both astrophysical black hole SgrA* and M87* and compare the results with Schwarzschild black hole lensing observables. In which we found that limiting value of angular position θ_∞ is smaller than Schwarzschild field limit black hole. Magnification μ is diverse when source position, β tends to zero. The separation between images s is larger than the Schwarzschild black hole.

Authors' Contributions

All authors have the same contribution.

Data Availability

The manuscript has no associated data or the data will not be deposited.

Conflicts of Interest

The authors declare that there is no conflict of interest.

Ethical Considerations

The authors have diligently addressed ethical concerns, such as informed consent, plagiarism, data fabrication, misconduct, falsification, double publication, redundancy, submission, and other related matters.

Acknowledgment

AS and DVS would like to thank the Council of Science and Technology, Uttar Pradesh (CST-UP) grant no CST/D-828 for financial support, and Bablu would like to thank CSIR for financial support through the CSIR-NET-JRF fellowship.

References

[1] A. Einstein, "Lens-Like Action of a Star by the Deviation of Light in the Gravitational Field", Science **84**(2188), 506 (1936). DOI: 10.1126/science.84.2188.506

[2] F. W. Dyson, A. S. Eddington and C. Davidson, "A Determination of the Deflection of Light by the Sun's Gravitational Field, from Observations Made at the Total Eclipse of May 29, 1919", Philos Trans. A Math. Phys. Eng. Sci. **220**(571-581), 291 (1920). DOI: 10.1098/rsta.1920.0009

[3] The Event Horizon Telescope Collaboration et al, "First M87 Event Horizon Telescope Results. I. The Shadow of the Supermassive Black Hole", The Astrophysical Journal Letters **875**(1), L1 (2019). DOI: 10.3847/2041-8213/ab0ec7

[4] The Event Horizon Telescope Collaboration et al, "First M87 Event Horizon Telescope Results. II. Array and Instrumentation", The Astrophysical Journal Letters **875**(1), L2 (2019). DOI: 10.3847/2041-8213/ab0c96

[5] The Event Horizon Telescope Collaboration et al, "First M87 Event Horizon Telescope Results. III. Data Processing and Calibration", The Astrophysical Journal Letters **875**(1), L3 (2019). DOI: 10.3847/2041-8213/ab0c57

[6] The Event Horizon Telescope Collaboration et al, "First M87 Event Horizon Telescope Results. IV. Imaging the Central Supermassive Black Hole", The Astrophysical Journal Letters **875**(1), L4 (2019). DOI: 10.3847/2041-8213/ab0e85

[7] The Event Horizon Telescope Collaboration et al, "First M87 Event Horizon Telescope Results. V. Physical Origin of the Asymmetric Ring", The Astrophysical Journal Letters **875**(1), L5 (2019). DOI: 10.3847/2041-8213/ab0f43

[8] The Event Horizon Telescope Collaboration et al, "First M87 Event Horizon Telescope Results. VI. The Shadow and Mass of the Central Black Hole", The Astrophysical Journal Letters **875**(1), L6 (2019). DOI: 10.3847/2041-8213/ab1141

[9] The Event Horizon Telescope Collaboration et al, "First M87 Event Horizon Telescope Results. VII. Polarization of the Ring", The Astrophysical Journal Letters **910**(1), L12 (2021). DOI: 10.3847/2041-8213/abe71d

[10] The Event Horizon Telescope Collaboration et al, "First M87 Event Horizon Telescope Results. VIII. Magnetic Field Structure near The Event Horizon", The Astrophysical Journal Letters **910**(1), L13 (2021). DOI: 10.3847/2041-8213/abe4de

[11] The Event Horizon Telescope Collaboration et al, "First M87 Event Horizon Telescope Results. IX. Detection of Near-horizon Circular Polarization", The Astrophysical Journal Letters **957**(2), L20 (2023). DOI: 10.3847/2041-8213/acff70

[12] K. S. Virbhadra and G. F. R. Ellis, "Schwarzschild black hole lensing", Phys. Rev. D **62**, 084003 (2000). DOI: 10.1103/PhysRevD.62.084003

[13] C. M. Claudel, K. S. Virbhadra and G. F. R. Ellis, "The Geometry of photon surfaces", J. Math. Phys. **42**, 818 (2001). DOI: 10.1063/1.1308507

[14] V. Bozza and L. Mancini, "Observing Gravitational Lensing Effects by Sgr A* with Gravity", Astrophys. J. **753**(1), 56 (2012). DOI: 10.1088/0004-637X/753/1/56

[15] S. Pietroni and V. Bozza, "The impact of gravitational lensing in the reconstruction of stellar orbits around Sgr A*", JCAP **2022**(12), 018 (2022). DOI: 10.1088/1475-7516/2022/12/018

[16] N. Tsukamoto, "Deflection angle of a light ray reflected by a general marginally unstable photon sphere in a strong deflection limit", Phys. Rev. D, **102**, 104029 (2020). DOI: 10.1103/PhysRevD.102.104029

[17] N. Tsukamoto, "Gravitational lensing in the Simpson-Visser black-bounce spacetime in a strong deflection limit", Phys. Rev. D **103**, 024033 (2021). DOI: 10.1103/PhysRevD.103.024033

[18] N. Tsukamoto, "Gravitational lensing by a photon sphere in a Reissner-Nordström naked singularity spacetime in strong deflection limits", Phys. Rev. D **104**, 124016 (2021). DOI: 10.1103/PhysRevD.104.124016

[19] C. Furtado, J. R. Nascimento, A. Y. Petrov, P. J. Porfírio and A. R. Soares, "Strong gravitational lensing in a spacetime with topological charge within the Eddington-inspired Born-Infeld gravity", Phys. Rev. D **103**, 044047 (2021). DOI: 10.1103/PhysRevD.103.044047

[20] V. A. Kosteleckỳ and R. Potting, "CPT and strings", Nucl. Phys. B **359**(2-3), 545 (1991). DOI: 10.1016/0550-3213(91)90071-5

[21] D. Colladay and V. A. Kosteleckỳ, "Lorentz violating extension of the standard model", Phys. Rev. D **58**, 116002 (1998). DOI: 10.1103/PhysRevD.58.116002

[22] V. A. Kosteleckỳ and S. Samuel, "Phenomenological Gravitational Constraints on Strings and Higher Dimensional Theories", Phys. Rev. Lett. **63**, 224 (1989). DOI: doi.org/10.1103/PhysRevLett.63.224

[23] R. Gambini and J. Pullin, "Nonstandard optics from quantum space-time", Phys. Rev. D **59**, 124021 (1999). DOI: 10.1103/PhysRevD.59.124021

[24] E. Battista, "Quantum Schwarzschild geometry in effective field theory models of gravity", Phys. Rev. D **109**, 026004 (2024). DOI: 10.1103/PhysRevD.109.026004

[25] V. A. Kosteleckỳ and S. Samuel, "Gravitational Phenomenology in Higher Dimensional Theories and Strings", Phys. Rev. D **40**, 1886 (1989). DOI: 10.1103/PhysRevD.40.1886

[26] M. Kalb and P. Ramond, "Classical direct interstring action", Phys. Rev. D **9**, 2273 (1974). DOI: 10.1103/PhysRevD.9.2273

[27] A. D. Sakharov, "The Initial Stage of an Expanding Universe and the Appearance of a Nonuniform Distribution of Matter", JETP **22**(1), 241 (1966).

[28] E. B. Gliner, "Algebraic Properties of the Energy-momentum Tensor and Vacuum-like States of Matter", JETP **22**(2), 378 (1966).

[29] J. Bardeen, "Non-singular general relativistic gravitational collapse" in Proceedings of GR5 (Tiflis, U.S.S.R., 1968).

[30] E. Ayon-Beato, A. Garcia, "The Bardeen model as a nonlinear magnetic monopole", Phys. Lett. B **493**(1-2), 149 (2000). DOI: 10.1016/S0370-2693(00)01125-4

[31] E. Ayon-Beato and A. Garcia, "Non-Singular Charged Black Hole Solution for Non-Linear Source", General Relativity and Gravitation **31**, 629 (1999). DOI: 10.1023/A:1026640911319

[32] E. Ayon-Beato and A. Garcia, "Four-parametric regular black hole solution", General Relativity and Gravitation **37**, 635 (2005). DOI: 10.1007/s10714-005-0050-y

[33] E. Ayon-Beato and A. Garcia, "Regular black hole in general relativity coupled to nonlinear electrodynamics", Phys. Rev. Lett. **80**, 5056 (1998). DOI: 10.1103/PhysRevLett.80.5056

[34] L. Xiang, Y. Ling and Y. G. Shen, "SINGULARITIES AND THE FINALE OF BLACK HOLE EVAPORATION", International Journal of Modern Physics D **22**(12), 1342016 (2013). DOI: 10.1142/S0218271813420169

[35] H. Culetu, "Nonsingular black hole with a nonlinear electric source", International Journal of Modern Physics D **24**(09), 1542001 (2015). DOI: 10.1142/S0218271815420018

[36] L. Balart and E. C. Vagenas, "Regular black holes with a nonlinear electrodynamics source", Phys. Rev. D **90**, 124045 (2014). DOI: 10.1103/PhysRevD.90.124045

[37] M. S. Ma, R. Zhao and Y. Q. Ma, "Thermodynamic stability of black holes surrounded by quintessence", General Relativity and Gravitation **49**(79), (2017). DOI: 10.1007/s10714-017-2245-4

[38] S. H. Hendi, S. Panahiyan and B. Eslam Panah, "Charged black hole solutions in Gauss-Bonnet-massive gravity", J. High Energy Phys. **2016**, 129 (2016). DOI: 10.1007/JHEP01(2016)129

[39] S. Ansoldi, "Spherical black holes with regular center: A Review of existing models including a recent realization with Gaussian sources", [arXiv:0802.0330 [gr-qc]].

[40] Md. Sabir Ali and S. G. Ghosh, "Exact d-dimensional Bardeen-de Sitter black holes and thermodynamics", Phys. Rev. D **98**, 084025 (2018). DOI: 10.1103/PhysRevD.98.084025

[41] A. Kumar, D. V. Singh and S. Upadhyay, "Impact of Perfect Fluid Dark Matter on the Thermodynamics of AdS Ayón–Beato–García Black Holes", JHAP **4**(4), 85 (2024). [arXiv:2503.04805v1 [gr-qc]].

[42] A. Kumar, D. V. Singh and S. Upadhyay, "Ayón–Beato–García black hole coupled with a cloud of strings: thermodynamics, shadows and quasinormal modes",Int. J. Mod. Phys. A **39**(31), 2450136 (2024). DOI: 10.1142/S0217751X24501367

[43] H. K. Sudhanshu, D. V. Singh, S. Upadhyay, Y. Myrzakulov and K. Myrzakulov, "Thermodynamics of a newly constructed black hole coupled with nonlinear electrodynamics and cloud of strings", Phys. Dark Univ. **46**, 101648 (2024). DOI: 10.1016/j.dark.2024.101648

[44] B. Singh, D. Veer Singh and B. Kumar Singh, "Thermodynamics, phase structure and quasinormal modes for AdS Heyward massive black hole", Phys. Scripta **99**(2), 025305 (2024). DOI: 10.1088/1402-4896/ad1da4

[45] P. Paul, S. Upadhyay, Y. Myrzakulov, D. V. Singh and K. Myrzakulov, "More exact thermodynamics of nonlinear charged AdS black holes in 4D critical gravity", Nucl. Phys. B **993**, 116259 (2023). DOI: 10.1016/j.nuclphysb.2023.116259

[46] D. V. Singh, A. Shukla and S. Upadhyay, "Quasinormal modes, shadow and thermodynamics of black holes coupled with nonlinear electrodynamics and cloud of strings", Annals Phys. **447**(1), 169157 (2022). DOI: 10.1016/j.aop.2022.169157

[47] D. V. Singh, S. G. Ghosh and S. D. Maharaj, "Exact nonsingular black holes and thermodynamics", Nucl. Phys. B **981**, 11584 (2022). DOI: 10.1016/j.nuclphysb.2022.115854

[48] D. V. Singh and S. Siwach, Phys. Lett. B **808**, 135658 (2020). DOI: 10.1016/j.physletb.2020.135658 [arXiv:2003.11754 [gr-qc]].

[49] V. Bozza, "Gravitational lensing in the strong field limit", Physical Review D **66**, 103001 (2002). DOI: 10.1103/PhysRevD.66.103001